A method for evaluating the microwave blackbody's equivalent brightness temperature by the Computational Fluid Dynamics simulation technologies

NIAN Feng[1, 2] , YANG Yujie[2], WANG Wei[1, 2]

1. *Science and Technology Laboratory on Metrology and Calibration Technology, Beijing* 100854, *China*;
2. *Beijing Institute of Radio Metrology and Measurement, Beijing* 100854, *China*

Abstract: The microwave calibration target's surface temperature is simulated using the computational fluid dynamics simulation technologies, which overcomes the difficulties of traditional methods in measuring the small wedge of calibration targets at a high precision. An evaluation method to calculate the calibration target's equivalent output temperature is introduced and the reference depth value of embedding the temperature sensor is applied, which efficiently reduces the difference between the sensor's measurement value and the calibration target's equivalent output temperature. The uncertainty of the calibration target's brightness temperature can be reduced within 0.5 K, which highly increases the measurement evaluation precision of the radiometer's calibration system.

Key words: calibration target, blackbody, brightness temperature, radiometer, microwave remote sensing

CLC number: TN98 **Document code:** A

Citation format: Nian F, Yang Y J and Wang W. 2011. A method for evaluating the microwave blackbody's equivalent brightness temperature by the Computational Fluid Dynamics simulation technologies. *Journal of Remote Sensing*, **15**(4): 687–695

1 INTRODUCTION

The microwave radiometers have been used as one of the main Earth observation and moon exploration instruments in our Fengyun series (FY-3), Haiyang series (HY-2) satellites and Shenzhou series, Change series spaceboat. The calibration of the microwave radiometer becomes one of the most important research in the microwave remote sensing domain (Nian, *et al.*, 2008; Wang, *et al.*, 2009; Mo, 1996; Jiang, *et al.*, 2008; Zhang, *et al.*, 2008; Li, *et al.*, 1999; Zhai, 2005). By now the microwave radiation international standard is still not being established (Randa, *et al.*, 2006), research on the microwave brightness standard and determination of the evaluation method of the outputing microwave brightness turns into a key issue.

Through the Project of Platform Construction on the FY-3 Meteorological Satellite Microwave Radiometer's Prelaunch Thermal/Vacuum Calibration, China have built the 10 GHz—200 GHz band microwave radiometer's calibration system, including the cold calibration targets, hot calibration targets and temperature variational calibration targets, standard antennas, the accurate temperature measurement and control system, and the blackbody emissivity measurement system to calibrate the microwave radiometer on orbit. Fig. 1 shows FY-3A thermal/vacuum calibration on microwave radiometers. The main function of the calibration targets is to output the standard microwave brightness T_B which makes microwave blackbody calibration targets with surface temperature $T(x, y, z)$ to radiate the microwave brightness T_B with the emissivity e near to 1. Therefore, the standard microwave radiation energy is projected onto the antenna to calibrate the radiometer. Fig. 2 shows the black calibration target (Nian & Wang, 2009). Because the calibration target's emissivity measurement is relatively mature, the key issue to determine the calibration target's outputing microwave brightness temperature T_B is focused on how to measure the surface temperature $T(x, y, z)$.

By now, only National Institute Standards and Technology (NIST) acquired the surface temperature distribution data by the infrared imager (Cox, *et al.* , 2006). However, the resolution of the

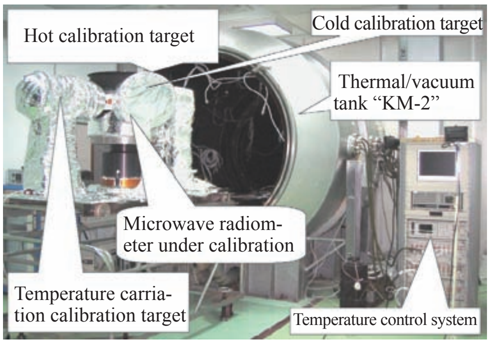

Fig. 1 The FY-3A's thermal/vacuum calibration experiment

Received: 2010-02-01; **Accepted**: 2011-02-26

First author biography: NIAN Feng (1974—), male, associate professor, postdoctor from the Second Academy of China Aerospace Science and Industry Corp. His research interests are electromagnetic simulation technology, active and passive radar detection technology. E-mail: nianfeng@m165.com

Fig. 2 The blackbody calibration target

present infrared imager is larger than 1 K, which can not be used to evaluate the calibration target's outputting brightness temperature accurately. How to acquire the calibration target's furface temperature distribution and how to research out an accurate brightness temperature method become the key points.

Furthermore, because of small scale of the calibration target wedge, for example, the wedge's bottom edge and height of the millimeter and calibration targets is about 10 mm and 50 mm, it is very difficult to lay down several thermal resistors along the small wedges to measure the surface temperature distribution. Thus it is necessary to determine an appropriate position for inserting the thermal resistors inside the blackbody wedges and keeping the thermal resistor's measurement value T_M and the equivalent temperature T_E of the wedges' surface temperature consistent with increase the measurement precision of the calibration target's surface temperature.

2 THE ANALYSIS ON THE THERMODYNAMICS CHARACTERISTICS OF THE CALIBRATION TARGETS

Thermal transmission has three ways: thermal conduction, thermal convection and thermal emission. The calibration targets have different thermal transmission ways for both ambient calibration and the vacuum calibration conditions. In the ambient calibration condition there exists all the three thermal transmission ways while only the thermal conduction and thermal emission in the vacuum calibration condition. The calibration target's wedge will show different surface temperature distribution in different calibration conditions.

There are contact and non contact methods to measure the object's surface temperature. The contact method realizes the temperature measurement by contacting the sensor, for example, Pt thermal resistor, sufficiently onto the object's surface. However, if the contact area is too small, the temperature measurement sensor will affect the temperature distribution due to the thermal conduction, which will lead to a serious measurement error. Because the calibration target's surface is relatively small compared with the present temperature measurement sensor, it is difficult to measure precisely. The non contact method mainly measures the infrared energy radiating from the object. This method is very suitable for measuring the calibration target wedge's surface temperature. However, the precision is about several K to tens K mainly used in insdutry's high temperature measurement domain which, in other words, is not sufficiently accurate to measure the calibration target on a milli K precision.

Applying the computational fluid dynamics (CFD) to calculate the calibration target's surface temperature is an efficiently method(Lakhkar, *et al.*, 2008; Tucker, 1997). Based on the CFD method, the calibration target's surface temperature is analyzed with the wedge's height to bottom edge ratio of 2 : 1, 4 : 1, 6 : 1, respectively, at the ambient and vacuum environment (Jackon & Gasiewski, 2000). The extreme condition of a wedge's base temperature, typically ranging from 80 K to 293 K environment background, is considered to acquire the extreme distribution of the calibration target's surface temperature. Fig. 3 shows the simulation results of the wedge's surface temperature distribution for the above conditions under ambient and vacuum environment. Table 1 shows the temperature of the wedge's top and the difference of the surface temperature (between the wedge's bottom and the top).

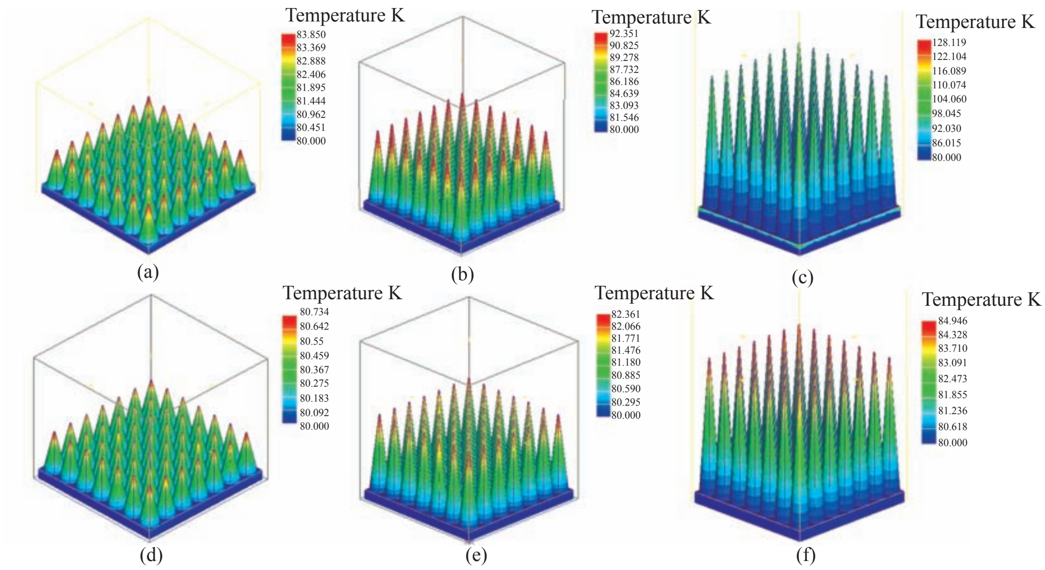

Fig.3 The calibration target's surface temperature distribution with different ratio of wedge's height to bottom edge in the ambient and vacuum environment (base temperature 80 K radiating to 293 K environment background)

(a)H/W= 2 : 1 under ambient environment; (b)H/W=4 : 1 under ambient environment; (c)H/W=6 : 1 under ambient environment; (d)H/W= 2 : 1 under thermal/vacuum environment; (e)H/W=4 : 1 under thermal/vacuum environment; (f)H/W=6 : 1 under thermal/vacuum environment

Table 1 The surface temperature difference for different wedges in both ambient and thermal/vacuum environment

The ratio of wedge's height to bottom edge	2 : 1	4 : 1	6 : 1
The wedge's peak temperature under ambient environment /K	83.85	92.37	128.12
The wedge's temperature difference under ambient environment /K	3.85	12.37	48.12
The wedge's peak temperature under thermal/vacuum environment /K	80.73	82.36	84.95
The wedge's temperature difference under thermal/vacuum environment /K	0.73	2.36	4.95

Because the top of calibration target's wedge can not be infinite thin, it is not applicable to express the calibration target's surface temperature with temperature difference between the wedge's bottom and the top. Otherwise, adopting the calibration target's equivalent surface temperature T_E and determining the height of H_E along the wedge corresponding to T_E can determine the position to embed the thermometric resistor to reduce measurement error. Fig. 4 shows the scanematic diagram of the T_E's evaluation method.

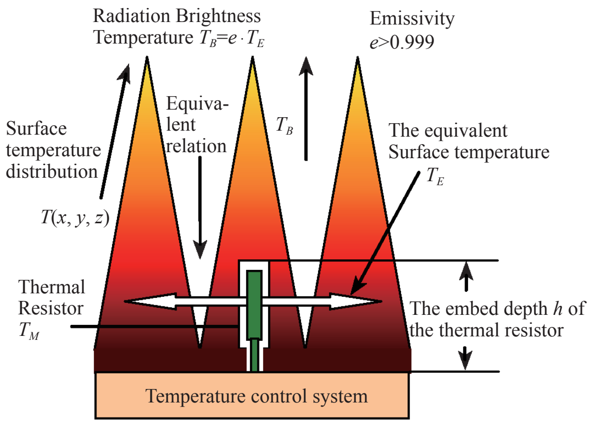

Fig.4 The diagram of the surface temperature distribution and the equivalent surface temperature evaluation method

3 THE EVALUATION METHOD FOR CALIBRATION TARGET'S EQUIVALENT OUTPUT BRIGHTNESS TEMPERATURE

The basic method to determine the calibration target's equivalent surface temperature can be followed by below procedures. Firstly, the surface temperature of the calibration target is discreted evenly. Secondly, the temperature in each of the discreted part is produced with the area of the corresponding discreted unit and then makes a summation of all the products. Finally, the calibration target's equivalent surface temperature T_E is obtained by dividing the summation by the overall surface area of the calibration targets. The calculation method is shown in Fig. 5. The calculation formula is

$$\begin{aligned} T_E &= \frac{1}{S}\iint_S T(x,y,z)\mathrm{d}s \\ &= \frac{1}{\pi (Nr)^2} \times \sum_{n=1}^{N} T_n \cdot \left\{\pi (nr)^2 - \pi\left[(n-1)r\right]^2\right\} \\ &= \frac{1}{N^2}\sum_{n=1}^{N} T_n \cdot (2n-1) \end{aligned} \tag{1}$$

where T_E——The equivalent temperature of the calibration target's wedge. S——The surface area of the calibra-tion target's wedge. $T(x, y, z)$——The surface temperature distribution of calibration target's wedge. N——The discreted number of the surface temperature on the calibration target. r——The projection width from the discreted surface to the bottom of the calibration target.

With Eq. (1) and based on the discretion method in Fig. 4, the equivalent output temperature is calculated as shown in Table 2.

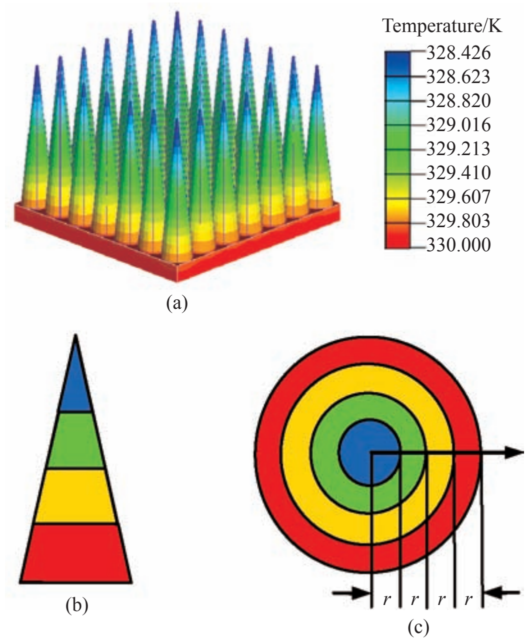

Fig.5 The diagram of the equivalent surface temperature calculation method of the calibration target's wedges
(a)The surface temperature distribution on the calibration target; (b)Side view of a wedge's surface temperature distribution; (c)Top view of a wedge's surface temperature distribution

Table 2 The equivalent temperature for different calibration target's wedges under ambient and thermal/vacuum environment

The ratio of wedge's height to bottom edge	2 : 1	4 : 1	6 : 1
The wedge's equivalent surface temperature under ambient environment /K	81.21	83.89	95.15
The wedge's equivalent surface temperature under thermal/vacuum environment /K	80.23	80.74	81.56

The position of the equivalent temperature on the calibration target's wedge under ambient and thermal/vacuum environments can be determined by the comparision with the temperature difference between the wedge's bottom temperature T_B and peak temperature T_P as Eq. (2).

$$H_E = \frac{T_E - T_B}{T_P - T_B} \times H_W \tag{2}$$

where H_E can be adopted as the control position to embed the thermal resistor for measuring the calibration target's surface equivalent temperature. With the calibration target been applied the ratio of H/W=4 : 1, the H_E of the base temperature with 80 K and 330 K radiating to 293 K background under ambient and thermal/vacuum environments are calculated as shown in Table 3.

Table 3 The position of the calibration target's surface equivalent temperature at the ratio of *H/W*=4 : 1

H/*W*=4 : 1	Base→background	Position of surface equivalent temperature
Ambient environment	80 K→293 K	37.7 mm
	330 K→293 K	37.8 mm
Thermal/vacuum environment	80 K→293 K	37.6 mm
	330 K→293 K	37.3 mm

From Table 3, the average position of the surface equivalent temperature is 37.6 mm, which can be used as the central position to embed the thermal resistor in both ambient and thermal/vacuum environments. Based on the above calculation, the uncertainty to measure the calibration target's surface temperature is mainly caused by the temperature measurement system. The uncertainty ΔT_E from the error of the position to embed the thermal resistor is less than 0.1 K. For a calibration target with emissivity e=0.995, the measurement uncertainty Δe is 0.001. The maxium uncertainty for the calibration target's outputing brightness temperature when T_E equals to 330 K can be calculated as Eq. (3).

$$\begin{aligned}\Delta T_B &= \Delta T_E \times e + T_E \Delta e \\ &= 0.1 \times 0.9995 + 330 \times 0.001 \\ &= 0.42\end{aligned} \tag{3}$$

With the uncertainty of the calibration target output brightness temperature is less than 0.5 K, the measurement accuracy has been improved greatly.

4 CONCLUSION AND DISCUSSION

(1)Adopting the CFD simulation to analysis the calibration target's surface temperature is the most efficient method by now. However, this method needs to be certified by the thermal/vacuum experiment, which a comparision between the CFD simulation with the measurement result for the different positions from the wedge's bottom to peak at 0, 1/4, 1/2 will be carried out to certify the correction of the simulated results.

(2)The CFD analysis shows that the surface temperature for different wedge's heights varies greatly, especially in the ambient environment with air convection. Therefore, the optimization design for the calibration target must consider the thermal characteristics apart from the electromagnetics. However, most of the former designs only emphasize the electromagnetics and neglect the thermal design.

(3)Due to the limited space, in many cases that only one thermal resistor can be embed inside one calibration target's wedge. So the thermal resistor's embeded position is very important to guarantee the measurement accuracy of the the calibration target's equivalent outputting temperature. Based on the analysis results of two ultimate conditions that 80 K and 330 K radiating to ambient and thermal/vacuum environment, our results show that the 1/4 position upper from the bottom of the calibration target's wedges is the most suitable measurement position for detecting the calibration target's equivalent temperature. Thus using this position to embed the thermal resistor is recommended.

(4)Combined with the present emissivity measurement accuracy level of calibration target and based on the above analysis results, a more higher accuracy level of the brightness temperature's uncertainty less than 0.5 K will be relized in the nearly future. This would keep us with the advanced level by the next step of thermal/vacuum calibration experiments and proper embeding the thermal resistor's position inside the calibration target's wedge.

REFERENCES

Cheng C Y, Wu C B, Zhai H and Chen Y M. 2006. Experimental study on emissivity measurement of 5mm blackbody. The 2006 4th Asia-Pacific Conference on Enviromental Electromagnetic: 644–647

Cox A E, Connell J J and Rice J P. 2006. Initial results from the infrared calibration target. IEEE International Conference on Geoscience and Remote Sensing Symposium, IGARSS 2006: 3463–3465

Jackon D M and Gasiewski A J. 2000. Electromagnetic and thermal analyses of radiometer calibration targets. Geoscience and Remote Sensing Symposium Proceedings, IGARSS 2000, 7: 2827–2829

Jiang J S, Wu Y R, Liu H G and Dong X L. 2008. New stage and new tasks, development of microwave remote sensing in China. *Engineering Sciences,* **10**(6):10–22

Lakhkar N, Hossain M and Agonafer D. 2008. CFD modeling of a thermoelectric device for electronics cooling applications. 11th Intersociety Conference on Thermal and Thermomechanical Phenomena in Electronic Systems: 889–895

Li J, Jiang J S and Li M T. 1999. Calibration of microwave radiometer. *Remote Sensing Techno-logy and Application*, **14**(1): 1–4

Mo T. 1996. Prelaunch calibration of the advanced microwave sounding Unit-A for NOAA-K. *IEEE Transactions on Microwave Theory and Techniques*, **44**(8): 1460–1469

Nian F, Yang Y J, Chen Y M, Xu D Z and Wang W. 2008. Recent progress on space borne microwave sounder prelaunch calibration technologies in China. *Journal of Systems Engineering and Electronics*, **19**(4): 643–651

Nian F, Yang Y J and Wang W. 2009. Research of optimizing the microwave wide band blackbody calibration target. *Journal of Systems Engineering and Electronics*, **20**(1): 6–12

Randa J, Cox A E and Walker D K. 2006. Proposed development of a national standard for microwave brightness temperature. IEEE International Conference on Geoscience and Remote Sensing Symposium, IGARSS 2006: 3996–3999

Randa J, Walker D K, Cox A E and Billinger R L. 2005. Errors resulting from the reflectivity of calibration targets. *IEEE Transactions on Geoscience and Remote Sensing*, **43**(1): 50–58

Tucker P G. 1997. CFD applied to electronic systems: a review. *IEEE Transactions on Components, Packaging, and Manufacturing Technology-Part A*, **20**(4): 518–529

Wang Z Z, Liu J Y, Yin X B and Jiang J S. 2009, Removing upwind/downwind ambiguity of ocean wind direction by polarimetric microwave radiometer: Scheme design on on-orbit calibration and scanning geometry. *Journal of Remote Sensing*, **13**(2): 190–196

Zhai H. 2005. The discussion on the key technology for microwave radiometer's calibration targets. The 15th National Academic Conference for Micro-wave Remote Sensing Technology: 59–60

Zhang S W, Li J, Jiang J S, Sun M H and Wang Z Z. 2008. Design and Development of Microwave Humidity Sounder for FY-3 Meteorological Satellite. *Journal of Remote Sensing*, **12**(8): 199–207

基于CFD技术的微波定标源亮温评定方法

年丰[1, 2]，杨于杰[2]，王伟[1, 2]

1. 计量与校准技术国防科技重点实验室，北京 100854；
2. 北京无线电计量测试研究所，北京 100854

摘 要：基于计算流体动力学仿真技术对微波定标源表面物理温度分布进行了仿真，解决了现有测温手段难以对小尺寸定标源尖劈进行高精度温度测量的问题，在此基础上建立了定标源等效输出物理温度的评定方法，并给出测温电阻埋设深度的建议值，从而有效减少测温电阻测量值与定标源等效表面物理温度值的差值，给出定标源输出亮温度不确定度小于0.5 K的合理评定结果，提高了微波辐射计定标系统的精度评估水平。

关键词：定标源，黑体，亮温，辐射计，微波遥感

中图分类号：TN98 **文献标志码**：A

引用格式：年丰，杨于杰，王伟．2011．基于CFD技术的微波定标源亮温评定方法．遥感学报，**15**(4)：687–695

Nian F, Yang Y J and Wang W. 2011. A method for evaluating the microwave blackbody's equivalent brightness temperature by the Computational Fluid Dynamics simulation technologies. *Journal of Remote Sensing*, **15**(4): 687–695

1 引 言

微波辐射计已成为中国风云系列卫星(FY-3)、海洋系列(HY-2)卫星以及神州系列、嫦娥工程探月卫星对地及探月观测的主要仪器，对微波辐射计进行精确标定是当前微波遥感仪器研究领域面临的重大课题之一(Nian 等，2008；Wang 等，2009；Mo，1996；姜景山 等，2008；张升伟 等，2008；李靖 等，1999；翟宏，2005)。目前国际上还尚未建立统一的微波辐射国际计量标准(Randa 等，2006)，研究微波亮温输出标准并给出精确的亮温输出值评价方法是解决这一课题的关键。

中国通过FY-3气象卫星微波辐射计发射前地面热真空定标条件建设项目初步建立了10 GHz—200 GHz频段由冷源、热源和变温源、标准天线、精密测温控温系统和空间法黑体发射率测量平台等构成的微波辐射计定标系统，主要用于对星上微波辐射计进行定标工作，图1为FY-3A热真空定标现场图。其中：定标源的主要功能是输出微波波段标准亮温度，即使表面温度为$T(x, y, z)$的微波黑体定标源以e接近于1的发射率辐射出指定频段的微波亮温度T_B，以提供标准的微波能量到微波辐射计天线/馈源口面用于对辐射计的整体标定。黑体定标源基体实物图如图2(Nian和Wang，2009)。

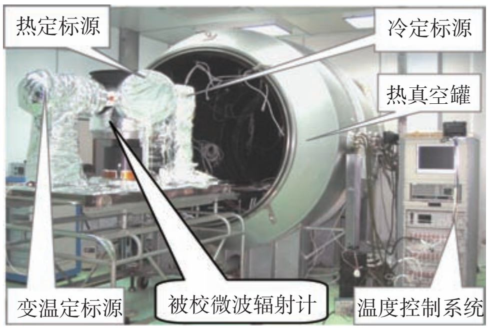

图1 FY-3A热真空定标试验现场图

图2 黑体定标源基体实物图

收稿日期：2010-02-01；**修订日期**：2011-02-26

基金项目：“FY-3”卫星微波有效载荷定标研制保障条件建设项目；国防科工局计量科研项目

第一作者简介：年丰（1974— ），男，博士，2007至2009年于航天科工集团第二研究院博士后流动站开展微波辐射计定标技术研究，主要研究领域为电磁场数值分析技术，主、被动微波探测技术。E-mail: nianfeng@m165.com。

由于定标源发射率e的测量方法较为成熟，因此准确地测量定标源的表面温度$T(x，y，z)$成为确定定标源输出标准亮温度T_B的关键。截至目前，仅有美国NIST(National Institute Standards and Technology)基于红外成像仪获得了定标源表面温度均匀性的分布情况(Cox 等，2006)，但红外成像仪观测精度目前还不能达到1 K以内，无法用于定标源输出亮温值的定量评估。因此如何获得定标源表面物理温度分布并研究准确的亮温评估方法成为本文的研究重点。

此外，由于定标源尖劈尺寸较小,例如毫米波段定标源尖劈底边宽度和高度为10 mm和50 mm左右，空间狭小，难以在尖劈内部高度方向敷设多个测温电阻对定标源尖劈表面温度分布进行测量，特别需要确定一个合理的测温电阻敷设高度，从而使测温电阻测量值T_m与定标源表面温度分布的整体等效值T_E非常接近，从而提高定标源表面物理温度的测量准确度。

2 定标源热力学特性分析方法

传热的3种基本方式为：热传导、热对流和热辐射。定标源在实验室定标条件下和真空定标条件下存在不同的传热现象。在实验室定标条件下3种方式都存在，真空定标条件下只存在热传导和热辐射。定标源两种条件下不同传热现象作用的结果将引起尖劈表面温度$T(x，y，z)$的不同分布。

目前物体表面温度测量的方法主要有接触式测量和非接触式测量：接触式测量需要通过测温传感器，如高精度铂测温电阻，与被测物体表面充分接触。但被测物体表面较小时，测温传感器本身会通过热传导影响被测物体表面的温度分布，造成测量结果会有较大误差。定标源尖劈面积较小，采用接触式测量很难准确地获得其表面的温度分布；非接触式测量主要通过测量被测物体表面辐射红外能量的方式来测量其表面温度，这种非接触测量方式在形式上非常适合测量定标源尖劈的表面温度分布，但是目前其测量精度较低，在几K至几十K数量级，主要用于工业界高温测量领域，目前还无法满足定标源的毫K级测量精度要求。

因此，本文采用计算流体动力学CFD(Computational Fluid Dynamics)数值仿真的方法是目前解决定标源表面温度分布的一种有效手段(Lakhkar 等，2008；Tucker，1997)。

本项目研究过程中采用CFD仿真方法首先对实验室和真空条件下定标源尖劈高度与底边比例为2∶1、4∶1和6∶1的定标源尖劈表面物理温度分布情况进行数值分析(Jackon和Gasiewski，2000)，并考虑到定标源尖劈表面温度分布的极限值情况，将基体底部温度设为80 K向环境背景温度为293 K时的传热情况。图3(a)—(f)为基体底部为80 K，环境背景为293 K时定标源不同尖劈高度底边长比例在实验室和热真空条件下尖劈表面温度分布仿真计算结果，表1为基体底部为80 K，环境背景为293 K时黑体定标源不同尖劈高度底边长比例在实验室和热真空条件下尖劈尖部温度值和表面

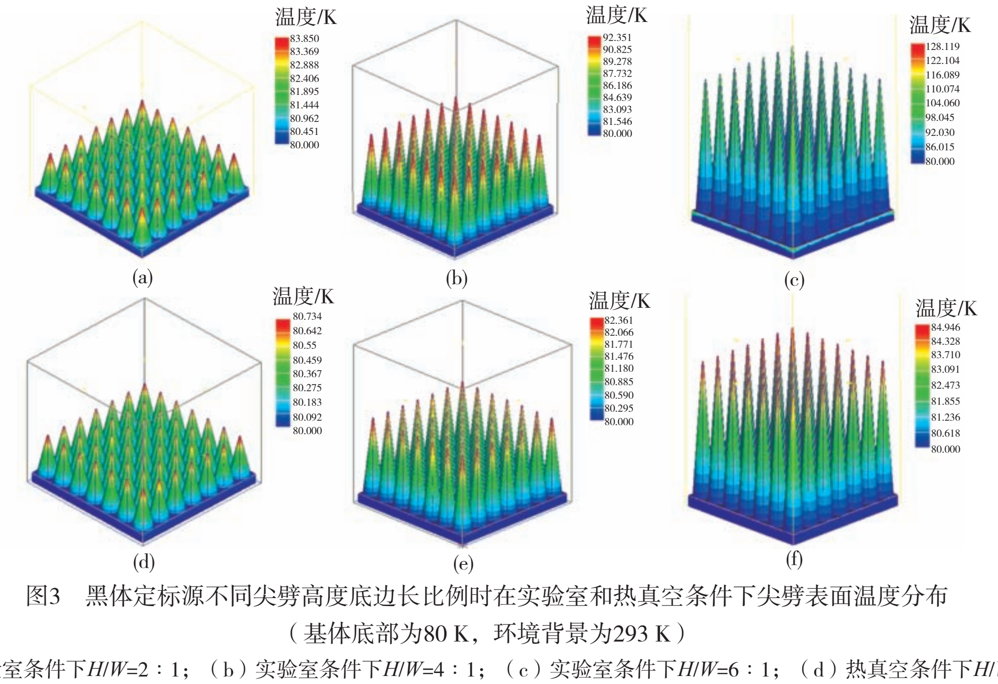

图3 黑体定标源不同尖劈高度底边长比例时在实验室和热真空条件下尖劈表面温度分布
（基体底部为80 K，环境背景为293 K）
（a）实验室条件下H/W=2∶1；（b）实验室条件下H/W=4∶1；（c）实验室条件下H/W=6∶1；（d）热真空条件下H/W=2∶1
（e）热真空条件下H/W=4∶1；（f）热真空条件下H/W=6∶1

温度差(基体底部和尖部之间的温度差值)数值列表。

表1　实验室和热真空条件下定标源不同尖劈尺寸表面温度差

尖劈高度底边长比例	2∶1	4∶1	6∶1
实验室条件下尖劈尖部温度/K	83.85	92.37	128.12
实验室条件下温度分布差/K	3.85	12.37	48.12
热真空条件下尖劈尖部温度/K	80.73	82.36	84.95
热真空条件下温度分布差/K	0.73	2.36	4.95

由于实际的黑体定标源尖劈顶部不能做到无限细，因此采用定标源基体底部和尖部之间的温度差值来表征定标源表面温度分布情况不具有实际意义。而确定定标源的等效表面物理温度T_E，并确定该等效表面物理温度值所对应定标源尖劈的高度位置$H_{等效}$，从而确定测温电阻埋设位置，以减少测温误差才更具有实际意义。等效表面物理温度评定方法原理图如图4。

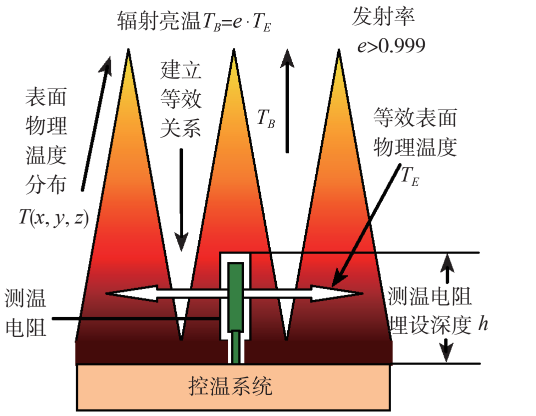

图4　黑体定标源表面物理温度分布与等效表面物理值确定原理图

3　定标源等效输出亮温评定方法

确定定标源等效表面温度值的基本方法是：对定标源表面温度分布沿尖劈表面进行等间隔离散，将每个等间隔段内的温度值与该间隔段内对应的面积值相乘，然后取和，再除以尖劈整体侧面表面积即为定标源等效表面温度T_E。计算方法如图5所示，计算公式如下：

$$T_E = \frac{1}{S_{尖劈表面积}} \iint_{S_{尖劈表面积}} T_{尖劈表面温度分布}(x,y,z)\mathrm{d}s = \frac{1}{\pi(Nr)^2}\sum_{n=1}^{N} T_n \times \left\{\pi(nr)^2 - \pi\left[(n-1)r\right]^2\right\} = \frac{1}{N^2}\sum_{n=1}^{N} T_n \times (2n-1) \tag{1}$$

式中，T_E为定标源尖劈表面等效温度值；$S_{尖劈表面积}$为圆锥尖劈侧表面积；$T_{尖劈表面温度分布}(x, y, z)$为尖劈表面温度分布；N为温度分布离散计算分段数目；r为温度分布离散计算段向尖劈底部投影的间隔宽度。

用式(1)和基于图4的离散化方法对图3的定标源进行等效输出亮温度计算，计算结果如表2所示。

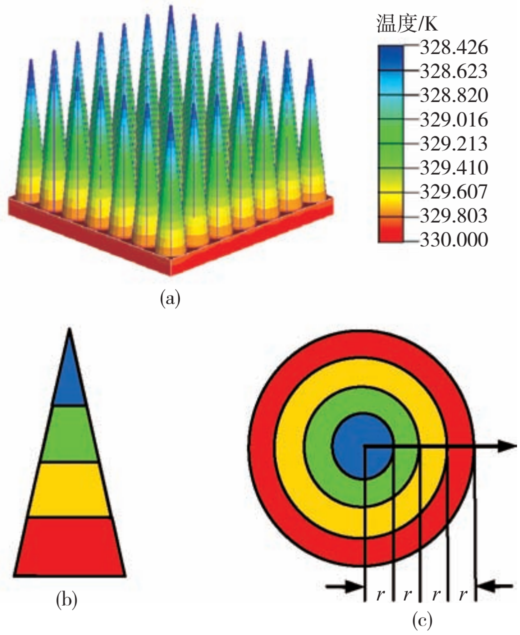

图5　定标源尖劈表面等效分布温度值计算方法示意图
(a)定标源尖劈表面温度分布；(b)单个尖劈表面温度分布侧视图；(c)单个尖劈表面温度分布俯视图

表2　实验室和热真空条件下定标源不同尖劈尺寸等效输出亮温度

尖劈高度底边长比例	2∶1	4∶1	6∶1
实验室条件下尖劈表面等效输出亮温度/K	81.21	83.89	95.15
热真空条件下尖劈表面等效输出亮温度/K	80.23	80.74	81.56

定标源尖劈在实验室和热真空条件下表面等效输出亮温度在尖劈底部向上的位置可通过对基体底部和尖部之间的温度差值进行比对计算获得，即：

$$H_{等效} = \frac{T_{等效} - T_{基体}}{T_{尖部} - T_{基体}} \times H_{尖劈} \tag{2}$$

此位置可作为在定标源尖劈内部放置测温电阻的敷设中心位置，由于本项目目前采用的黑体定标源尖劈高度底边长比例全部为H/W=4∶1，故最终仅对基体温度分别为80 K和330 K向293 K背景换热时在实验室条件和热真空条件下尖劈表面等效输出亮温度位置值进行计算，如表3。

表3 黑体定标源尖劈尺寸比例H/W= 4：1时表面等效输出亮温度位置

H/W=4：1	基体→背景温度	等效输出亮温度位置
实验室条件下	80 K→293 K	37.7 mm
	330 K→293 K	37.8 mm
热真空条件下	80 K→293 K	37.6 mm
	330 K→293 K	37.3 mm

对表3的等效输出亮温度位置取平均值为37.6 mm，此位置即可作为定标源尖劈高度底边长比例H/W=4：1时，实验室条件和热真空条件下在定标源尖劈内部放置测温电阻的敷设中心位置。此时，定标源尖劈表面输出亮温度的测量不确定度基本取决于测温系统的测量不确定度，而由测温位置带来的测量不确定度ΔT_E基本可以控制在0.1 K以内，对于定标源发射率e为0.9995，测量不确定度Δe为0.001，定标源T_E为330 K时，定标源输出亮温度不确定度可由式(3)计算得到

$$\begin{aligned}\Delta T_B &= \Delta T_E \times e + T_E \Delta e \\ &= 0.1 \times 0.9995 + 330 \times 0.001 \\ &= 0.42\end{aligned} \tag{3}$$

即定标源输出亮温度不确定度小于0.5 K，从而有效提高了定标源输出亮温度的精度。

4 结 论

(1)本文基于CFD数值分析方法，对获得黑体定标源尖劈表面物理温度分布非常有效，但其精度需要进一步通过热真空试验验证，在后续热真空定标实验中将采用在尖劈从根部向上0、1/4和1/2比例高度处埋设测温电阻，将测量值与CFD结果比对，以充分证明评定方法的准确性。

(2)通过热力学CFD分析发现，不同尖劈高度比例的表面温度差别较大，特别是在实验室有空气对流的情况尤为严重，对定标源输出亮温范围影响很大，因此对尖劈高度比例的设计必须兼顾其热力学特性，而以往通常以电磁学(发射率)设计为主，这方面应该引起重视。

(3)由于尖劈内部空间所限，一个尖劈内部只能埋设一个测温电阻，并且其埋设位置对定标源输出等效物理温度值的测量结果影响较大，本文通过80 K和330 K两个热真空定标极限温度向同一背景辐射的CFD分析结果，证明在尖劈根部向上1/4位置处为等效输出物理温度最佳测量位置，建议今后定标源采用此位置测温。

(4)结合目前定标源发射率测量精度水平和本文分析结果，可以预计通过下一轮定标实验、合理布设测温电阻位置，可使黑体定标源输出亮温度不确定度小于0.5 K。

REFERENCES

Cheng C Y, Wu C B, Zhai H and Chen Y M. 2006. Experimental study on emissivity measurement of 5mm blackbody. The 2006 4th Asia-Pacific Conference on Enviromental Electromagnetic: 644–647

Cox A E, Connell J J and Rice J P. 2006. Initial results from the infrared calibration target. IEEE International Conference on Geoscience and Remote Sensing Symposium, IGARSS 2006: 3463–3465

Jackon D M and Gasiewski A J. 2000. Electromagnetic and thermal analyses of radiometer calibration targets. Geoscience and Remote Sensing Symposium Proceedings, IGARSS 2000, 7: 2827–2829

Jiang J S, Wu Y R, Liu H G and Dong X L. 2008. New stage and new tasks, development of microwave remote sensing in China. *Engineering Sciences,* **10**(6):10–22

Lakhkar N, Hossain M and Agonafer D. 2008. CFD modeling of a thermoelectric device for electronics cooling applications. 11th Intersociety Conference on Thermal and Thermomechanical Phenomena in Electronic Systems: 889–895

Li J, Jiang J S and Li M T. 1999. Calibration of microwave radiometer. *Remote Sensing Technology and Application*, **14**(1): 1–4

Mo T. 1996. Prelaunch calibration of the advanced microwave sounding Unit-A for NOAA-K. *IEEE Transactions on Microwave Theory and Techniques*, **44**(8): 1460–1469

Nian F, Yang Y J, Chen Y M, Xu D Z and Wang W. 2008. Recent progress on space borne microwave sounder prelaunch calibration technologies in China. *Journal of Systems Engineering and Electronics*, **19**(4): 643–651

Nian F, Yang Y J and Wang W. 2009. Research of optimizing the microwave wide band blackbody calibration target. *Journal of Systems Engineering and Electronics*, **20**(1): 6–12

Randa J, Cox A E and Walker D K. 2006. Proposed development of a national standard for microwave brightness temperature. IEEE International Conference on Geoscience and Remote Sensing Symposium, IGARSS 2006: 3996–3999

Randa J, Walker D K, Cox A E and Billinger R L. 2005. Errors resulting from the reflectivity of calibration targets. *IEEE Transactions on Geoscience and Remote Sensing*, **43**(1): 50–58

Tucker P G. 1997. CFD applied to electronic systems: a review. *IEEE Transactions on Components*, *Packaging, and Manufacturing Technology-Part A*, **20**(4): 518–529

Wang Z Z, Liu J Y, Yin X B and Jiang J S. 2009, Removing upwind/downwind ambiguity of ocean wind direction by polarimetric microwave radiometer: Scheme design on on-orbit calibration and scanning geometry. *Jounal of Remote Sensing*, **13**(2): 190–196

Zhai H. 2005. The discussion on the key technology for microwave radiometer’s calibration targets. The 15th National Academic Conference for Micro-wave Remote Sensing Technology: 59–60

Zhang S W, Li J, Jiang J S, Sun M H and Wang Z Z. 2008. Design and Development of Microwave Humidity Sounder for FY-3 Meteorological Satellite. *Journal of Remote Sensing*, **12**(8): 199–207

附中文参考文献

姜景山，吴一戎，刘和光，董晓龙. 2008. 中国微波遥感发展的新阶段新任务. 中国工程科学，**10**(6)：10–22

李靖，姜景山，李茂堂. 1999. 微波辐射计定标. 遥感技术与应用，**14**(1)：1–4

翟宏. 2005. 微波辐射计定标源关键技术探讨. 第15届全国微波遥感技术学术交流会：59–60

张升伟，李靖，姜景山，孙茂华，王振占. 2008. 风云3号卫星微波湿度计的系统设计与研制. 遥感学报，**12**(8)：199–207